

# Enhancing Bond Strength of 3D-Printed Resin Posts Using Various Surface Pretreatments: An In Vitro Study

Cihan Küden, DDS, PhD

Department of Endodontics, Faculty of Dentistry, Cukurova University, Adana, Turkey.

Sevde Gül Batmaz, DDS

Seda Nur Karakaş, DDS


Department of Restorative Dentistry, Faculty of Dentistry, Cukurova University, Adana, Turkey.

**Purpose:** This study investigated the impact of common surface pretreatments on the contact angle (CA), surface free energy (SFE), and push-out bond strength (PBS) of custom 3D-printed resin posts. **Materials and Methods:** Post spaces of 60 endodontically treated mandibular premolars were prepared. Custom 3D-printed posts made from permanent crown resin were fabricated for 50 randomly selected post spaces. The specimens were then divided into six groups (n = 10) based on their surface pretreatment methods. These methods included sandblasting (SB), silane (SL), hydrofluoric acid (HF), and hydrogen peroxide (HP). Additionally, two control groups were established: glass fiber control (GFC) and permanent resin control (PRC). CA and SFE were measured for each 3D-printed post group. PBS and failure mode analyses were conducted. The data were analyzed using the two-way ANOVA followed by the Tukey post hoc test ( $\alpha = .05$ ). **Results:** The lowest CA values were found in the SB and SL groups. The SB group had the highest SFE compared to all other groups. SL markedly enhanced the PBS of the resin post compared to the PRC at the cervical, middle, and apical levels ( $P = .001$ ,  $P = .000$ , and  $P = .002$ , respectively), and the values were comparable to those of the GFC ( $P = .695$ ,  $P = .999$ , and  $P = .992$ , respectively). Except in the GFC, SB, and SL groups, mixed failure decreased from the cervical to apical levels, while adhesive failure rates increased. **Conclusions:** The application of silane and sandblasting to the surfaces of custom 3D-printed resin posts effectively increased their SFE, thereby enhancing their adhesion. *Int J Prosthodont* 2024;37(suppl):s253–s263. doi: 10.11607/ijp.8914

Post-core restorations play a crucial role in dispersing intraoral forces from the crown to the root, extending into the radicular dentin. This process strengthens the overall tooth structure, particularly in teeth that were treated endodontically and exhibit loss of coronal substance.<sup>1,2</sup> The mechanical properties of the post materials used should closely align with those of dentin to achieve these goals.<sup>3</sup> However, the absence of a universally accepted material or technique for ideal post-core restorations is noteworthy.<sup>4</sup> The use of inappropriate materials or techniques may increase the risk of tooth structure fracture or cause failure of the restoration.<sup>5,6</sup> In this context, glass fiber posts have emerged as a popular choice in dentistry due to their ease of use, esthetic appeal, and an elastic modulus similar to that of dentin.<sup>7</sup> Despite these advantages, glass fiber posts can induce mechanical stress at the cervical area and

Correspondence to:  
Dr Cihan Küden,  
ckuden@cu.edu.tr

Submitted October 30, 2023;  
accepted February 20, 2024.  
©2024 by Quintessence  
Publishing Co Inc.



restoration boundaries, often leading to inadequate tooth structure reinforcement.<sup>8</sup> Furthermore, prefabricated fiber posts present clinical limitations, including bonding failures and adaptation challenges,<sup>9</sup> especially in elliptical root canals.<sup>10</sup> The gap between the dentin and these posts can result in an uneven resin cement layer, causing increased polymerization shrinkage, stress, and eventual post failure.<sup>6,9,10</sup>

The dearth of comprehensive data pertaining to the optimal material and dimensions for post cores has prompted scholarly investigation into novel materials within this domain. According to existing literature, custom-cast posts and cores have been found to exhibit enhanced adaptation in comparison to prefabricated posts.<sup>4,9–11</sup> Additionally, they demonstrate the ability to conform to the walls of the radicular post space.<sup>12</sup> Custom posts offer several advantages compared to prefabricated post-and-core systems. These advantages include increased resistance to rotational forces, a higher success rate, and improved removability for endodontic retreatment.<sup>9,11</sup> Computer-aided design (CAD) and additive manufacturing (AM) techniques are increasingly recognized as convenient, evolving, and contemporary methods for the fabrication of custom post cores.<sup>10,13–15</sup> In contrast to subtractive manufacturing, the utilization of AM avoids the use of burs or drills, thereby eliminating issues related to wear and allowing for the effortless printing of intricate geometries.<sup>16</sup> Additionally, this method significantly reduces material waste by producing only the required objects.<sup>17</sup> This technique involves creating 3D objects through the sequential photopolymerization of thin resin layers and uses various methods in the 3D printing production process, such as stereolithography (SLA) and digital light processing (DLP).<sup>18–20</sup> A range of materials such as gold alloys, titanium alloys, base metal alloys, zirconia, and polymeric-based materials can be utilized in the fabrication process of custom 3D-printed posts and cores. The existing literature reveals that zirconia materials exhibit low bonding with resin cement.<sup>14</sup> Additionally, it was reported that titanium and zirconia custom posts, while demonstrating high flexural strength,<sup>21</sup> may lead to root fractures due to their higher flexural modulus compared to dentin.<sup>14,21</sup> Therefore, polymeric materials are gaining prominence due to their bonding capabilities with resin cement, a flexural modulus that closely mirrors that of dentin, and their cost-effectiveness.<sup>22,23</sup> A particularly noteworthy resin-based material is the recently developed permanent crown resin (Formlabs), which is produced using AM techniques and exhibits an elastic modulus closely mirroring that of dentin.

The effectiveness of a post-core restoration depends critically on the selection of materials and the integrity of interfaces among materials with varying compositions.<sup>24</sup> Ensuring proper adhesion at the interface between the

post and composite resin is crucial for the effective distribution of stresses generated by occlusion.<sup>25</sup> Also, a correlation has been shown between the bond strength of surface-treated posts and adhesive resin cements and the contact angle (CA) and surface free energy (SFE) properties of these materials.<sup>26,27</sup> Various pretreatment techniques have been suggested to enhance bond strength, such as acidic solution etching,<sup>5,28</sup> silanization,<sup>4,24,29,30</sup> hydrogen peroxide,<sup>24,30</sup> and sandblasting etching.<sup>30–33</sup> However, there is a lack of information regarding the use of 3D-printed customized posts as the dental post material and appropriate surface pretreatments. Simultaneously, the literature does not present a consensus regarding an established surface pretreatment for a particular post-core material. Although research indicates that silanization improves bonding,<sup>4,29</sup> studies also suggest that its impact may not be significant.<sup>31,34</sup> Hence, the objective of this research was to examine the impact of surface pretreatments commonly employed in conjunction with 3D-printed resin posts on the CA, SFE, and push-out bond strength (PBS). The null hypothesis of the study presumed that there would be no significant differences in terms of CA, SFE, and PBS among 3D-printed custom posts subjected to various surface pretreatments.

## MATERIALS AND METHODS

The present study obtained ethical approval from the Non-Invasive Clinical Research Ethics Committee of the Faculty of Medicine at Cukurova University, with the assigned reference number 2022/126-31. The current in-vitro study utilized mandibular premolar teeth extracted from patients at the Surgery Clinic of the Faculty of Dentistry, Çukurova University. The extractions were indicated for orthodontic or periodontal reasons, and patients provided informed consent to participate in the study.

### Sample Size Calculation

According to a prior investigation,<sup>35</sup> a power analysis was conducted using G\*Power 3.1 (Heinrich Heine University, Düsseldorf, Germany) to ascertain the minimum sample size required for each group. The analysis aimed to achieve a power of 85%, an alpha level of .05, and an effect size of 0.53. The determined minimum sample size for each group was eight. Consequently, a total of 10 samples were employed for each group in this in-vitro investigation.

### Preparation of the Root Canals

Sixty caries-free human mandibular premolar teeth without root curvature and possessing one root and one canal were utilized in this study (n = 10). The root surfaces of the teeth were cleaned of any calculus and

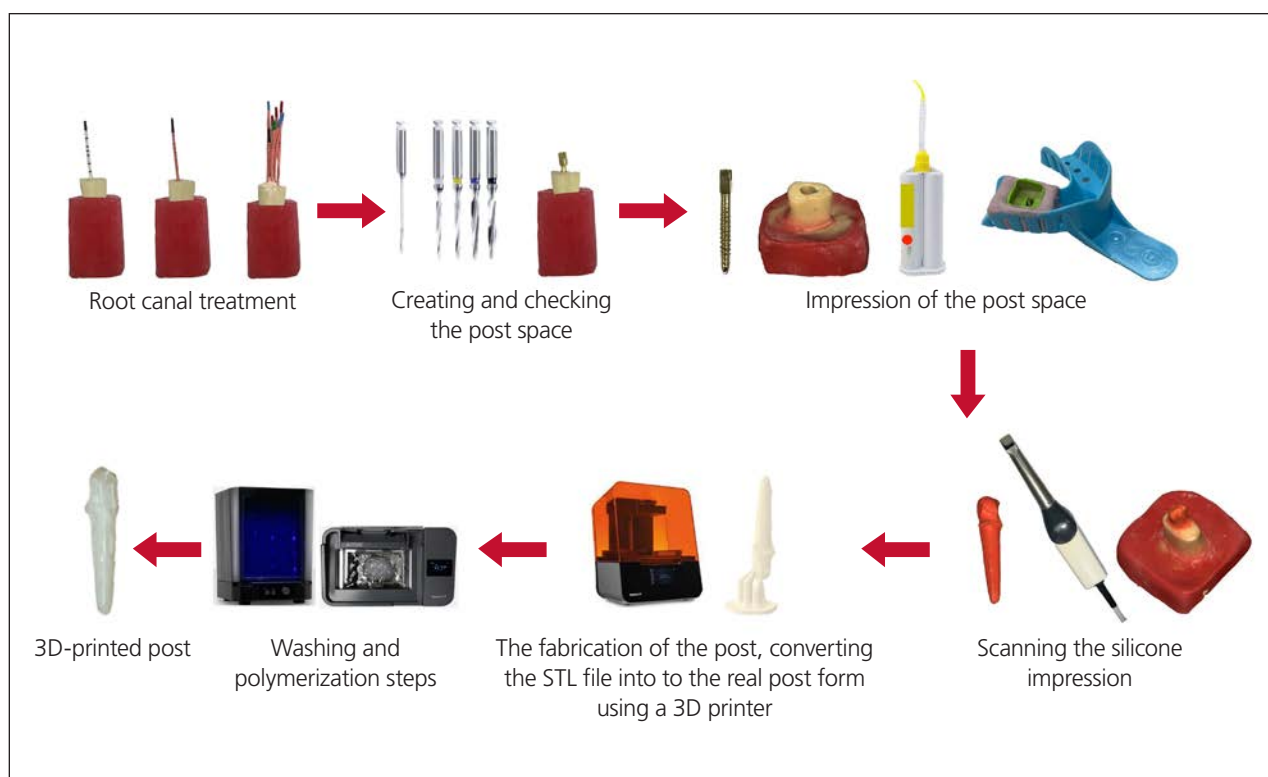


**Fig 1** Representation of the stages in the preparation of a custom 3D-printed permanent crown resin post.

periodontal tissue residues using a piezoelectric ultrasonic device (Ultrawave, Ultradent). The teeth were subjected to examination using a stereomicroscope (Olympus SZ61, Olympus Optical Co) at a magnification of 40 $\times$ . This examination aimed to identify the presence of any cracks, fractures, abrasion, erosion, or resorption in the teeth. Defective teeth were replaced with suitable ones. The teeth exhibited comparable characteristics in terms of root morphology, length, and width and were preserved in a solution containing 0.1% thymol. To standardize the teeth, they were cut to 14-mm root lengths using a diamond separator with water cooling. The working length of the root canal was established as 1 mm less than the position of the apical foramen utilizing a #10 K-type file. The shaping of root canals was conducted utilizing Reciproc R25 and R40 reciprocal files (VDW) operated by a torque-limited electric motor (VDW). Following every three pecking motions, the root canals were irrigated using a total volume of 15 mL of distilled water per root canal. The procedure of root canal obturation was executed utilizing the cold lateral condensation technique, employing gutta-percha and an epoxy-based resin root canal sealer known as AdSeal (MetaBiomed). The efficacy of root canal treatment was verified by means of periapical radiographs. The root canal orifices were sealed using a temporary filling material (Cavit, 3M ESPE). All root canal treatment


stages were performed by the same operator (C.K.). The samples were subjected to incubation conditions of 37°C and 95% relative humidity for 1 week.

#### Preparation and Impression of the Post Space

The post cavity preparation was conducted using Gates-Glidden and post drills (Cytec blanco, Hahnenkratt), following the method described in the study by Küden et al.<sup>36</sup> Post space impressions were obtained following the method of Piangsuk et al.<sup>9</sup> Polyvinyl siloxane putty and light body (Express, 3M ESPE), an impression tray, and a post were used to obtain impressions of the post space. Light-body silicone was used to fill the post space initially, followed by the placement of the metal post. After obtaining the impression, the length of the impression and the post space were verified using a hand file.

#### Production of Resin Posts by 3D Printing

The post impression was scanned using a dental laboratory scanner (inEos X5, Dentsply Sirona). The resulting data, in STL (standard tessellation language) format with a resolution of 50 microns (Fig 1), were transferred to a 3D printer (Formlabs), and post structures were fabricated using permanent crown resin material (Formlabs). Subsequently, the samples were washed with 99% pure isopropyl alcohol in a Form Wash device (Formlabs) for 5 minutes and polymerized in a Form Cure device



(Formlabs) at 60°C for 20 minutes. Each printed post was subjected to a sequential sanding procedure using sandpapers of varying grit sizes: 600, 1,200, and 2,400. Subsequently, the specimens were polished via a 90-second treatment using Impomza pumice (Imicryl) at a rotational speed of 1,500 rpm. Following this process, the samples were thoroughly cleansed in an ultrasonic bath for 1 minute and then allowed to air dry.

### Groups According to the Post Surface Pretreatment

The samples were randomly divided into six groups based on surface pretreatment: glass fiber post as a control group (GFC), permanent crown resin as a control group (PRC), sandblasting (SB), silane (SL), hydrofluoric acid (HF), and hydrogen peroxide (HP). No pretreatment was applied to the glass fiber post (Cytec blanco) and 3D-printed post surface in the GFC and PRC groups, respectively. In the SB group, the 3D-printed post surface was subjected to sandblasting using aluminum oxide particles with a diameter of 110  $\mu\text{m}$  (Rocatec Pre powder, 3M ESPE). The sandblasting process was conducted at a distance of 1 cm for a duration of 30 seconds, with a pressure of 2.8 bar. Following sandblasting, the samples were cleaned in an ultrasonic cleaner and dried. In the SL group, silane (Ultradent) was applied to the 3D-printed post surface with an applicator for 60 seconds and then dried. In the HF group, the 3D-printed post surface was acidified with 9% HF (Ultradent) for 60 seconds and rinsed with distilled water for 60 seconds.<sup>27</sup> In the HP group, HP of 24% was applied to the 3D-printed post surface for 60 seconds and rinsed with distilled water for 60 seconds.<sup>25</sup>

### CA and SFE Analysis

To determine the SFE using angle measurements, 10 samples from each of the four surface pretreatment groups as well as from the PRC group were prepared, each measuring 2 mm in thickness, 2 mm in length, and 2 mm in width. The surface wettability of resin samples with varying surface pretreatments was assessed through CA measurements conducted using the sessile drop method. Liquids with distinct polarities, including distilled water, ethylene glycol, and dimethyl sulfoxide, were utilized for this evaluation. Three drops (0.4- $\mu\text{L}$  drop volume for each liquid) were placed on each material surface used in this study. The CAs between liquids with different hydrophobicity values and the surfaces of the materials were obtained using a computer-aided CA-measuring device (OCA-50, Dataphysics Instruments).

Average CA values were used to calculate the SFE, and the calculations were performed according to the approach presented by van Oss et al.<sup>37</sup> The total SFE (or  $\gamma\text{ST}$ ) value was determined by adding the dispersive ( $\gamma\text{SD}$ ) and polar  $\gamma\text{SP}$ ) components.

### Cementation of Posts

The posts utilized in this study underwent a cleaning process involving the use of 70% ethanol and subsequent air drying. The cementation of the posts was performed using RelyX U200 (3M ESPE). The resin cement was prepared in accordance with the guidelines provided by the manufacturer. Subsequently, the posts were coated with resin cement and carefully inserted into the post space using manual finger pressure. The removal of surplus cement was accomplished by means of a cotton pellet. The samples underwent polymerization by using an LED light device (Valo, Ultradent) for a duration of 40 seconds. Following polymerization, the samples were submerged in distilled water at a temperature of 37°C for 1 week. The cementation order was random and the cementation procedure was performed by an experienced operator.

### PBS Test

Each specimen was embedded in clear acrylic resin. The specimens were subjected to a precision cutting process using the Accutom 10 device (Struers) to obtain sections with a thickness of 1 mm. These sections were taken from the coronal, middle, and apical thirds of the root for each specimen. The dimensions of the coronal, middle, and apical post sections, including their diameters and thicknesses, were assessed using a digital caliper (HSL 246–15, Karl Hammacher GmbH). The post sections were subjected to testing using a universal testing device (Testometric M500, 25 kN). The loading process was carried out at a cross-head rate of 0.5 mm/min using a metal rod appropriate for the diameter of the post section. The test continued until failure of the post section was observed. Bond strength values were determined employing the formula and computational methodology used in Küden et al<sup>36</sup> study.

### Failure Mode Analysis

The categorization of failure modes was conducted using a stereomicroscope (Olympus SZ61) at a magnification of 40 $\times$ . The consensus was reached by two trained and calibrated operators. The sections were divided into three distinct classifications<sup>14</sup> due to the occurrence of three modes of failure in the fiber posts: type 1 = adhesive failure between the post and the resin cement; type 2 = mixed failure, partially covering the post section and the resin cement; type 3 = cohesive failure within the fiber post.

### Scanning Electron Microscopy Analysis

A fiber post and 3D-printed posts with the different surface pretreatments were randomly selected to represent the post groups. The prepared posts were affixed to aluminum stubs and subjected to a gold sputter coating. The post surfaces were analyzed utilizing scanning



electron microscopy (SEM; FEI, Quanta 650 FEG). The images were acquired at magnifications of  $\times 1,000$  and  $\times 10,000$ .

### Randomization and Statistical Analysis

All randomization procedures, including the assignment of teeth to experimental groups, the cementation process, push-out testing, fracture type examination, and the selection of SEM images, were conducted using the GraphPad QuickCalcs program (GraphPad). The data were analyzed using a statistical program (SPSS, IBM). The Shapiro-Wilk test was utilized to determine the normal distribution of the evaluated data. The analysis of the PBS, CA, and SFE values was conducted using two-way ANOVA and Tukey tests. The ratio of failure mode was computed for each group. The data was evaluated utilizing a confidence interval of 95% ( $\alpha = .05$ ).

## RESULTS

### CA

The CA mean values, standard deviations, and statistical differences of all materials are presented in Fig 2. The groups with the lowest CA values were SB (67.71 degrees) and SL (70.74 degrees). A statistically significant difference ( $P = .000$ ) was observed between these groups and other experimental groups. The groups with the highest water CA values were HP (97.21 degrees) and HF (95.52 degrees), which were found to be statistically significantly higher than the PRC group ( $P = .000$ ).

### SFE

The mean SFE values and standard deviations of the groups are presented in Fig 3. The dispersive component ( $\gamma_{SD}$ ) contributes significantly more to SFE, while the contribution of the polar component ( $\gamma_{SP}$ ) is comparatively lower.

For the  $\gamma_{SP}$  component, the SB and SL groups showed no significant difference between them ( $P = .999$ ), and they exhibited the lowest  $\gamma_{SP}$  component values among all the groups. Statistically significant differences were observed between the SB group and the PRC, HF, and HP groups ( $P = .002$ ,  $P = .001$ , and  $P = .012$ , respectively). Similarly, significant differences were also found between the SL group and the PRC, HF, and HP groups ( $P = .003$ ,  $P = .001$ , and  $P = .013$ , respectively).

The SB group exhibited the highest SFE ( $\gamma_{ST}$ ) with a recorded value of 72.54, and this value demonstrates statistical significance when compared to all other groups ( $P = .000$  for all pairwise comparisons except SL;  $P = .024$  for SB and SL comparison). There was no statistically significant distinction observed between the HF and HP groups ( $P = .901$ ). However, it is worth noting that both the HF and HP groups exhibited significantly higher  $\gamma_{ST}$  values in comparison to the PRC group ( $P = .000$ ).

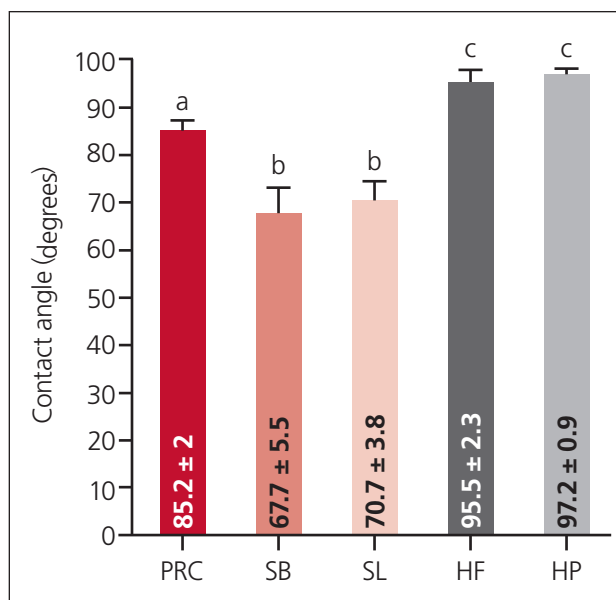


**Fig 2** Contact angle. The mean CA values and their standard deviations for the PRC group and the groups subjected to different surface pretreatments are displayed at the bottom of the bars. Different letters show the statistical differences among the groups ( $\alpha = .05$ ).

The statistical difference in the  $\gamma_{SD}$  values among the groups is exactly the same as the statistical differences among the  $\gamma_{ST}$  values.

### PBS

The average and standard deviation values of the experimental groups are shown in Fig 4. Two-way ANOVA showed that the pretreatment method and root region were factors affecting PBS ( $P = .000$  and  $P = .000$ , respectively). However, there was no interaction between root region and pretreatment on the PBS ( $P = .124$ ).

In the cervical region, the GFP group demonstrated the highest PBS value. A statistically significant difference was noted between the GFP group and the others ( $P = .001$  for SB and  $P = .000$  for PRC, HF, and HP), except for the SL group ( $P = .695$ ). The SL group exhibited a significantly higher PBS value compared to the PRC, HF, and HP groups ( $P = .001$ ,  $P = .000$ , and  $P = .000$ , respectively). There was no significant difference between the SL and SB groups ( $P = .052$ ), and there were no statistically significant differences observed between the SB group and the PRC, HF, and HP groups ( $P = .647$ ,  $P = .188$ , and  $P = .086$ , respectively).

In the middle region, the PBS value of the SL group was the highest. Significant statistical differences were observed when the SL group was compared to the PRC, SB, HF, and HP groups ( $P = .000$ ,  $P = .002$ ,  $P = .000$ , and  $P = .000$ , respectively). Similarly, the GFP group exhibited significantly higher PBS value than the PRC, SB, HF, and HP groups ( $P = .000$ ,  $P = .001$ ,  $P = .000$ , and  $P = .000$ ,

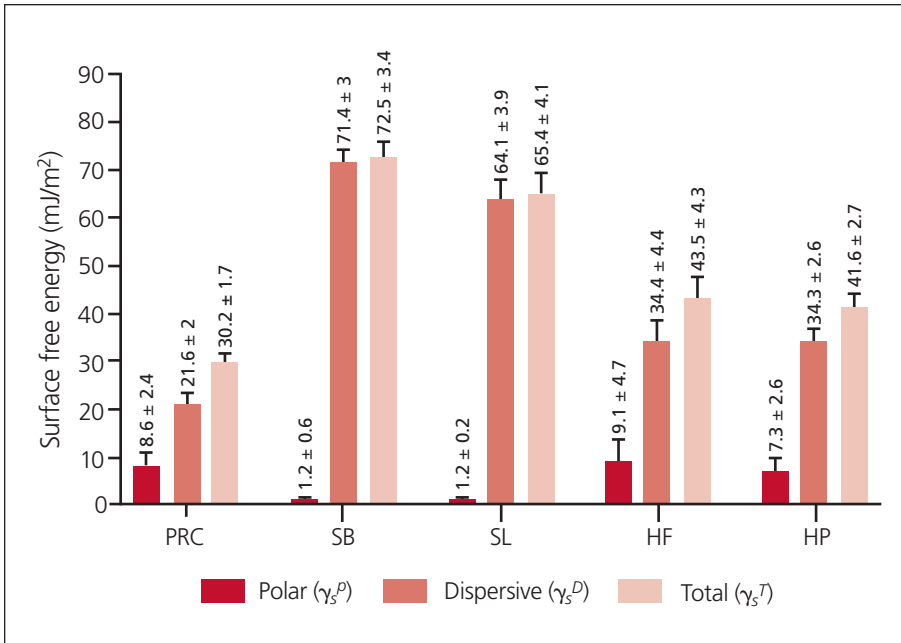


**Fig 3** Surface free energy. The mean SFE values and their standard deviations for the PRC group and the groups subjected to different surface pretreatments are displayed above the bars.

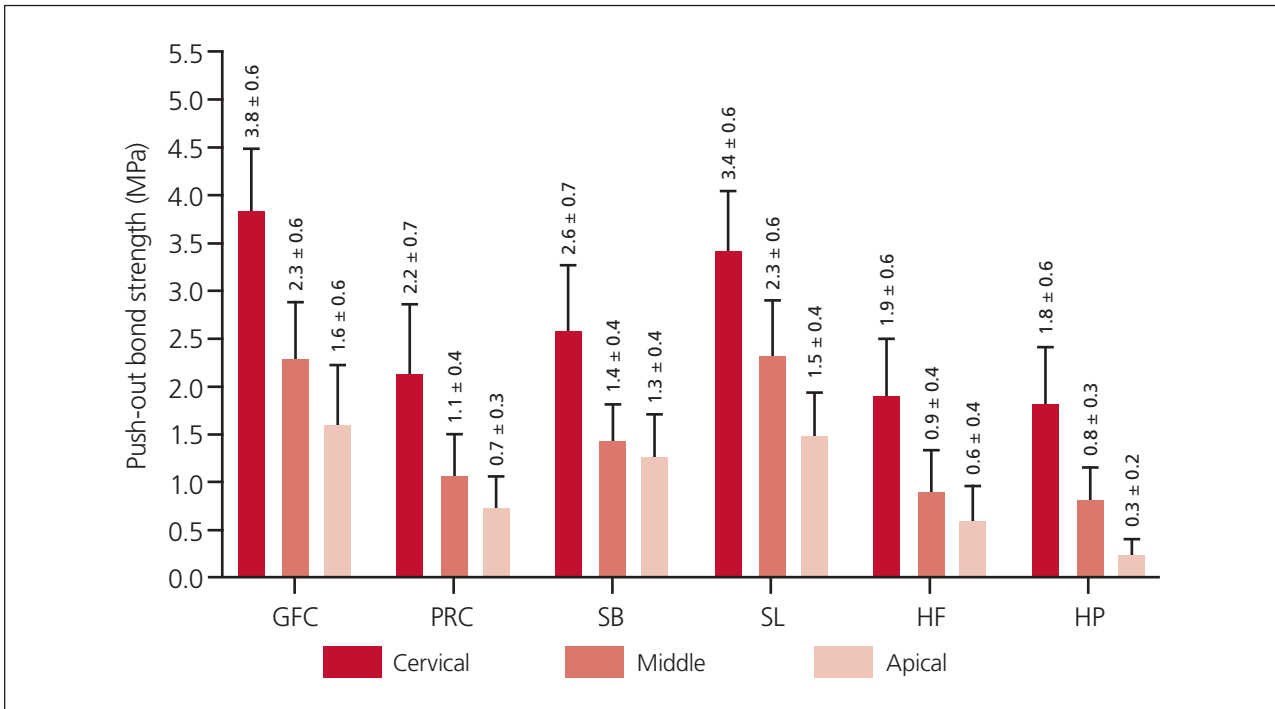


**Fig 4** Push-out bond strength. The PBS mean values and their standard deviations of the groups are displayed above the bars. The different colors of the bars represent different regions of the root canal: cervical, middle, and apical.

respectively). There was no significant difference between the GFC and SL groups ( $P = .999$ ), and there was no significant difference between the PRC group and the SB, HF, and HP groups ( $P = .505$ ,  $P = .965$ , and  $P = .858$ ).

In the apical region, the GFC and SL groups demonstrated significantly higher PBS values compared to the other groups, except for the SB group ( $P = .000$ ). There

was no significant difference between the PRC group and the SB, HF, and HP groups ( $P = .062$ ,  $P = .973$ , and  $P = .126$ , respectively).

When comparing different regions of root canals among the groups, decreasing PBS values from cervical to apical regions were observed in all groups. PBS values of root regions in the GFC, SL, and HP groups differed



from each other. In the GFC group, differences were observed between the cervical and middle regions and between the middle and apical regions ( $P = .000$  and  $P = .045$ , respectively). Similarly, differences between the cervical and middle regions and between the middle and apical regions were also noted in the SL group ( $P = .000$  and  $P = .007$ , respectively) and in the HP group ( $P = .000$  and  $P = .012$ , respectively). In the PRC, SB, and HF groups, the cervical section demonstrated significantly higher PBS values than the other two sections ( $P = .000$ ), but there was no significant difference between the middle and apical sections of these groups ( $P = .345$ ,  $P = .771$ , and  $P = .344$ , respectively).

### Failure Mode

The failure mode rates of the groups are shown in Fig 5. The percentage of mixed failure occurring from cervical to apical decreased except for the GFC, SB, and SL groups. In the cervical region, adhesive failure rates remained below 50% for all groups, while in the middle region, adhesive failure rates were above 50% for the PRC, HF, and HP groups. In the apical region, adhesive failure rates were 50% and above in all groups.

The highest cohesive failure rate was observed in the GFC group in the cervical part, and cohesive failure was also observed in the same part in the SL and SB groups. For the apical region, cohesive failure was observed in the SL and GFC groups with a rate of 10%.

### SEM

Representative SEM images at  $\times 1,000$  and  $\times 10,000$  magnification of the GFC and PRC groups and posts made of resin with different surfaces applied to their surfaces are shown in Fig 6. The general appearance of serrated fiber rods is clearly observed in the GFC group. In this respect, this group displayed the roughest surface morphology. SEM evaluation revealed that the post surface morphology of posts produced from resin material changed compared to the control group after different surface pretreatments. HF and HP groups showed similar SEM images, exhibiting a perforated and corroded surface appearance. SB, however, created the roughest surface after the GFC group, especially at  $\times 1,000$  magnification. However, grains of sand remaining on the surface are observed in the  $\times 10,000$  SEM images. The SL group showed a similar appearance to the PRC group at  $\times 1,000$ , while it showed a rougher surface structure at  $\times 10,000$ .

## DISCUSSION

In the current study, post restorations for endodontically treated teeth were uniquely produced for each canal using permanent crown resin material and the 3D printing method. Subsequently, the study focused on

evaluating the effects of various surface pretreatment protocols on the CA, SFE, and PBS of these 3D-printed posts. The results of the study indicated that the surface pretreatments significantly affected the CA, SFE, and PBS of the posts, thereby leading to the rejection of the null hypothesis.

Various authors have proposed new digital technology-based methods for post and core fabrication,<sup>10,13</sup> yet these innovative techniques lack thorough investigation. Although digital workflows and technology have been suggested to yield post-and-core systems comparable to traditional methods,<sup>15</sup> the literature offers limited insight into potential enhancements. Hence, this study utilized AM within a digital workflow to produce customized posts for each root canal, also evaluating the effects of surface pretreatments on the adhesion to the root canal.

CAD and AM techniques are increasingly prominent in dentistry for personalized production. Notably, AM generates less waste compared to subtractive methods.<sup>17</sup> Vat polymerization in AM, which encompasses SLA and DLP, is widely employed in dental applications due to its superior structural resolution, excellent surface quality, and satisfactory z-axis strength.<sup>18</sup> SLA involves vertical build platform movement along the z-axis and horizontal laser movement in the xy plane to trigger polymerization of light-sensitive resin at a specific point. In SLA 3D printing, a laser beam is employed to create and cure each layer's pattern in light-curable resin. DLP technology, similar to SLA, uses micro mirror arrays to simultaneously polymerize monomers across a complete layer.<sup>19</sup> SLA offers notable advantages, including speed, resistance to temperature, and the ability to print intricate geometric forms.<sup>20</sup> Consequently, the 3D-printed posts in this study were produced using the SLA method for these reasons.

The clinical success of post-core restorations depends on material selection and the quality of interfaces between materials with differing compositions.<sup>24</sup> Achieving proper adhesion at the post-composite resin interface is crucial for effective stress distribution.<sup>25</sup> Surface chemistry alterations, affecting SFE, have a significant impact on bond strength.<sup>38</sup> This study measured CAs of polar and nonpolar liquids to evaluate surface wettability, with a focus on assessing surface hydrophilicity using the water CA. Enhanced wettability of dental material surfaces is essential for improved adhesion, as it allows a larger area.<sup>23</sup> To ensure clinical feasibility, this study selected commonly used surface pretreatments (silane, sandblasting, HF, and HP) based on factors like availability, applicability, and chairside procedure duration.<sup>24,25,31</sup> Studies demonstrated that surface pretreatments on glass fiber posts enhance surface wettability, resulting in increased SFE and, consequently, improved bonding.<sup>5,26,38</sup> In this study, it was observed that groups with a lower CA and higher SFE exhibited higher PBS values.

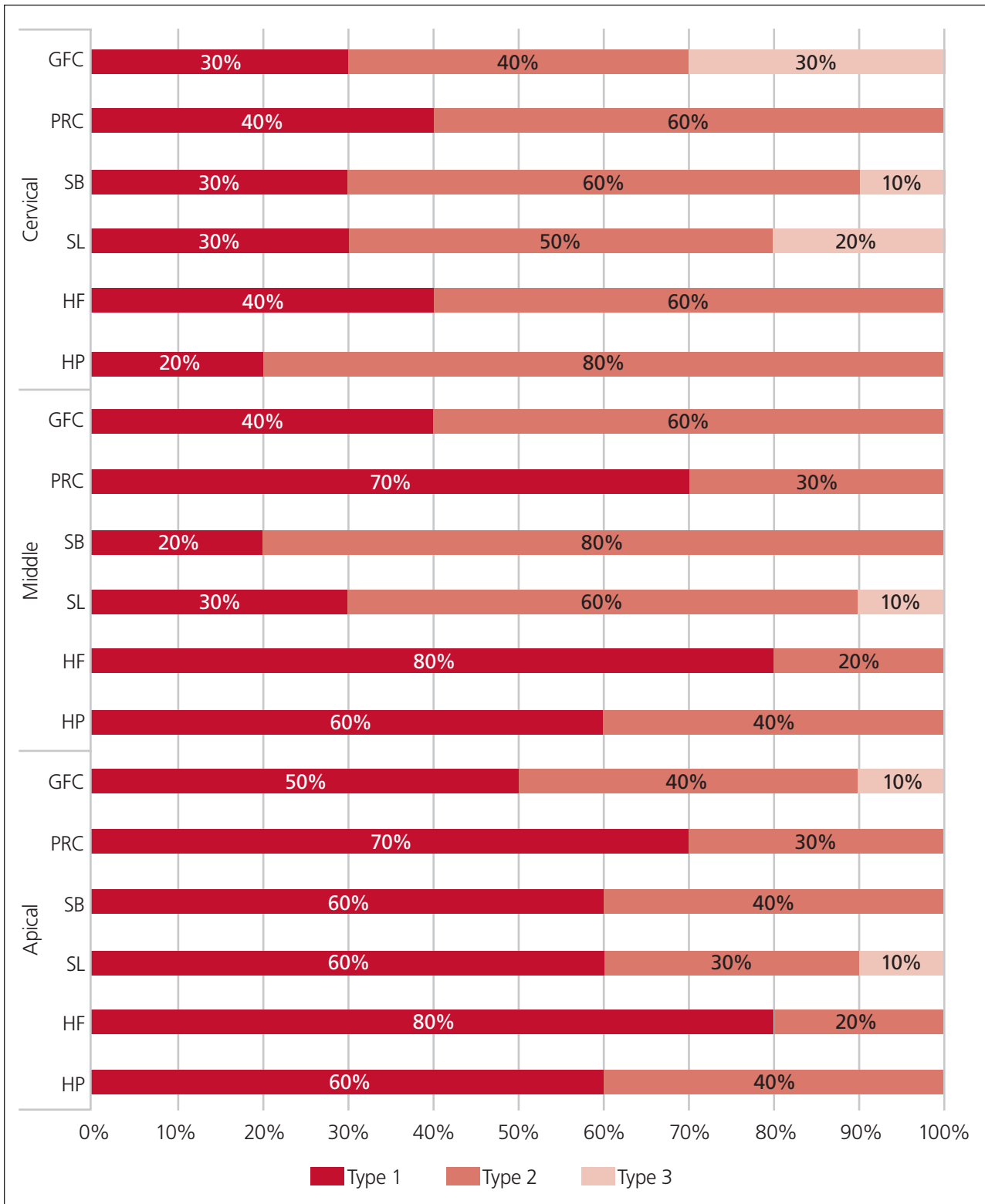


**Fig 5** The ratios of fracture pattern of the experimental groups. The fracture types are adhesive, mixed, and cohesive, respectively.

Silane is commonly employed as a surface pretreatment for fiber posts, altering the microstructure and roughness of the post's surface without notable modification. Silane application creates a "molecular bridge"

between inorganic and organic interfaces, improving the material surface's wettability. This molecular bridge effectively strengthens the bond at the interface between two different materials.<sup>5</sup> The mechanism of silane action



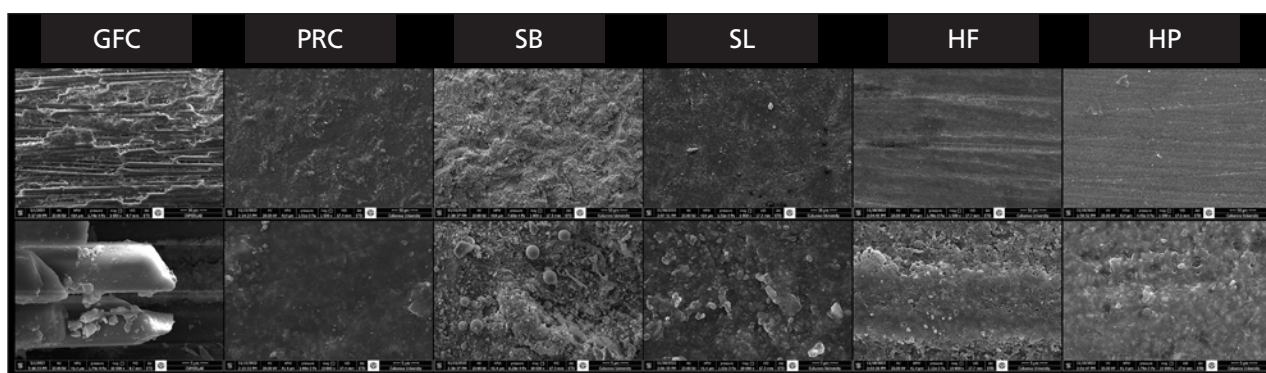


**Fig 6** Representative SEM images of the groups at magnifications of  $\times 1,000$  (top row) and  $\times 10,000$  (bottom row).

involves the formation of bonds between its functional alkoxy groups and OH-covered inorganic substrates. Silane establishes a chemical bridge with OH-coated substrates, such as carbon-based materials like resin-matrix composites.<sup>30,31</sup> Silane application on 3D-printed resin posts improved bond strength, aligning with previous research on fiber glass posts.<sup>4,24,29,30</sup> However, no prior studies were found on surface pretreatments for 3D-printed custom posts. Leme et al<sup>29</sup> and Zicari et al<sup>4</sup> studied the effect of silane on adhesion between fiber posts and RelyX U100 cement, a previous version of the cement used in this study. Both studies found that applying silane pretreatment improved the bond between the post and resin cement. In this study, silane pretreatment improved the PBS of 3D-printed posts. Upon measuring CAs, silane-treated samples showed lower values compared to the control group, suggesting increased hydrophilicity. This reduced CA facilitated adhesion to the resin cement, which is hydrophobic after polymerization. The enhanced SFE suggests that silane may form a chemical bond with the resin cement, potentially strengthening the bond.

Sandblasting is commonly used to enhance adhesion by creating surface roughness. This process involves airborne-particle abrasion, which generates a micro-textured surface, thereby increasing roughness and the available surface area for improved adhesion.<sup>31</sup>

Air abrasion with aluminum oxide ( $\text{Al}_2\text{O}_3$ ) particles enhances the endodontic post's roughness and augments the surface contact area, facilitating the flow of resin-matrix cement and mechanical interlocking under light-curing conditions.<sup>31</sup> Air-abraded fiber post surfaces are capable of significantly improving the polymer surface's CA, markedly boosting bond strength.<sup>31</sup> Sandblasting the surface of glass fiber posts significantly improved the retention of posts cemented with dual-cured resin cement.<sup>32</sup> Liu et al<sup>31</sup> utilized SEM imaging to demonstrate that the sandblasted rough surface of fiber posts exposed more fibers. They assumed that this sandblasting technique expanded the bonding area,

consequently establishing robust micromechanical interlocking. D'Arcangelo et al<sup>33</sup> recommended light sandblasting using  $50\text{-}\mu\text{m}$   $\text{Al}_2\text{O}_3$  particles as an approach to treat the fiber post surface. In this study, air abrasion with  $50\text{-}\mu\text{m}$   $\text{Al}_2\text{O}_3$  particles was performed, resulting in decreased CA and elevated SFE on the 3D-printed post surfaces, suggesting potential bond strength improvements. However, SEM images raised concerns about the presence of sand particles on the rough surface and their potential negative impact on the bond.

The effect of the hydrogen peroxide (HP) pretreatment on adhesion is attributed to the oxidation of the post surface, the partial removal of epoxy resin, and its bonding to resin cement.<sup>3</sup> Several studies have provided evidence that HP can effectively dissolve epoxy resin in fiber posts without causing damage to the glass fibers.<sup>39–41</sup> However, other studies proposed that HP did not affect the bond strength achieved, and in some cases, it may even have a detrimental effect on it.<sup>24,42</sup> The effect of bleaching agents on the bond strength between composites was studied by Ferrari et al,<sup>43</sup> and the results indicated that the use of 35% HP did not yield a statistically significant increase in composite-to-composite bond strength when compared to the control group that was not subjected to bleaching. They suggested that due to the porosity of the composite resin, residual HP and oxygen byproducts could act as potential reservoirs. This residual oxygen could inhibit the polymerization of the resin and consequently decrease the composite-to-composite bond strength.<sup>43</sup> This finding could be a possible explanation for why HP did not significantly affect the PBS value of the 3D-printed post in the present study, despite increasing the surface energy of the HP group compared to the PRC group.

Given that the silica and quartz found in fiber posts can be chemically equated with ceramic materials, the recent suggestion is to use hydrofluoric acid (HF) for the abrasion of these fiber posts. This procedure aims to form a roughened pattern on the surface, allowing for microscale mechanical interlocking between

the resin-matrix cement and the composite.<sup>5</sup> While HF pretreatment enhances surface texture, it carries the risk of potentially damaging the glass fibers, compromising post structural integrity.<sup>28</sup> The application of HF did not result in improved bond strength between the resin-matrix composite and glass fiber-reinforced resin composite posts.<sup>5,31</sup> In the present study, no significant change was observed in the bonding of the 3D-printed posts treated with HF. Upon analysis of the SEM images, there was no noticeable abrasion on the post surface. Similar to the HP group, the HF group also exhibited an increase in SFE compared to the PRC group. However, it demonstrated a significantly higher CA than the PRC group, which may elucidate the ineffectiveness of the HF application.

The analysis of bond strength across three root sections revealed that the cervical third was the most resilient, followed by the middle third, and lastly the apical third. Furthermore, upon comparison with other sections of the root canal, it is anticipated that both the diameter and density of the dentinal tubules are more considerable in the cervical third. Additionally, dentin hybridization is not uniform, and generally no tags form in the apical region of the root canal,<sup>44</sup> suggesting that this should result in decreased adhesion.<sup>45</sup> In this study, the most prevalent type of failure encountered was adhesive failure, subsequently followed by mixed failure. Considering the resin post-cement-dentin interface, mixed failure is deemed more favorable compared to adhesive failure. However, when taking into account the shaping of the intracanal void, the thickness of the resin-matrix cement layer tends to increase progressively from the apical to the coronal region.<sup>5,6</sup> In this study, the production of 3D-printed custom posts, which are tailored for each tooth based on its canal shape, resulted in the observation that the resin cement thickness is slimmer compared to the prefabricated posts. This observation is postulated to contribute to the higher incidence of adhesive failures.

Among the limitations of this study is its in-vitro nature, which cannot perfectly replicate the conditions of the oral environment. The data from this in-vitro study does not precisely predict the in-vivo performance of 3D-printed custom resin posts. This study evaluated the effect of a single printing orientation performed at 90 degrees on the CA, SFE, and PBS. The effect of different printing angles on PBS can be investigated in future studies. Although efforts were made to standardize the post space by using permanent mandibular premolar teeth, radicular dentin tubule diameter and density are among the factors that cannot be controlled. In this study, CA, SFE, and SEM were utilized to analyze PBS values resulting from various post surface pretreatments. To further investigate the changes induced by these surface pretreatments, future studies could explore the extent of surface roughness using techniques such as

atomic force microscopy or 3D profilometry. While a limitation arises from the absence of similar studies in the literature comparing surface pretreatments of 3D-printed resin posts, this gap also underscores the unique contribution and strength of the current research.

## CONCLUSIONS

Within the constraints of this study, custom posts produced by the 3D printing technique using permanent crown resin material showed that the application of silane and sandblasting enhanced the SFE, thereby improving adhesion. However, the use of HP and HF pretreatments did not result in a significant change in either the SFE or the adhesion strength.

## ACKNOWLEDGMENTS

The authors would like to thank Dr Orhun Ekren for his support. This research was supported by the Scientific Research Projects of Cukurova University (project number TSA-2022-14432), and the authors would especially like to thank the prosthetic laboratory for their support of this study.

All methods performed in the present study involving biologic material were in accordance with the ethical standards of the institutional and/or national research committee and with the 1964 Helsinki Declaration and its later modifications or comparable ethical standards. The present study and protocol were found medically appropriate according to the Clinical Research Ethics Committee report numbered 2022/126-31 of Cukurova University Faculty of Medicine.

The authors have no conflicts of interest to declare.

## REFERENCES

1. Chuang S-F, Yaman P, Herrero A, Dennison JB, Chang CH. Influence of post material and length on endodontically treated incisors: An in vitro and finite element study. *J Prosthet Dent* 2010;104:379-388.
2. Da Silva NR, Raposo LHA, Versluis A, Fernandes-Neto AJ, Soares CJ. The effect of post, core, crown type, and ferrule presence on the biomechanical behavior of endodontically treated bovine anterior teeth. *J Prosthet Dent* 2010;104:306-317.
3. Lamichhane A, Xu C, Zhang FQ. Dental fiber-post resin base material: A review. *J Adv Prosthodont* 2014;6:60-65.
4. Zicari F, De Munck J, Scotti R, Naert I, Van Meerbeek B. Factors affecting the cement-post interface. *Dent Mater* 2012;28:287-297.
5. Souza JC, Fernandes V, Correia A, et al. Surface modification of glass fiber-reinforced composite posts to enhance their bond strength to resin-matrix cements: An integrative review. *Clin Oral Investig* 2022;26:95-107.
6. Fernandes V, Silva AS, Carvalho O, et al. The resin-matrix cement layer thickness resultant from the intracanal fitting of teeth root canal posts: An integrative review. *Clin Oral Investig* 2021;25:5595-5612.
7. de Almeida Goncalves LA, Vansan LP, Paulino SM, Neto MDS. Fracture resistance of weakened roots restored with a transilluminating post and adhesive restorative materials. *J Prosthet Dent* 2006;96:339-344.
8. Schmitter M, Rammelsberg P, Lenz J, Scheuber S, Schweizerhof K, Rues S. Teeth restored using fiber-reinforced posts: In vitro fracture tests and finite element analysis. *Acta Biomater* 2010;6:3747-3754.
9. Piangasuk T, Henprasert P, Boonsiriphant P, Lindquist TJ. The accuracy comparison of 3D-printed post and core using castable resin and castable wax resin. *J. Prosthodont* 2023;32:540-545.



10. Farah RI, Aloraini AS, Al-Haj Ali SN. Fabrication of custom post-and-core using a directly fabricated silicone pattern and digital workflow. *J Prosthodont* 2020;29:631–635.
11. Fernandes AS, Shetty S, Coutinho I. Factors determining post selection: A literature review. *J Prosthet Dent* 2003;90:556–562.
12. Goto Y, Nicholls JL, Phillips KM, Junge T. Fatigue resistance of endodontically treated teeth restored with three dowel-and-core systems. *J Prosthet Dent* 2005;93:45–50.
13. Kanduti D, Korat L, Kosec T, Legat A, Ovsenik M, Kopač I. Comparison between accuracy of posts fabricated using conventional, CAD/CAM milling and 3D-printing techniques. *Appl Sci* 2022;12:11896.
15. Piangsuk T, Dawson DV, El-Kerdani T, Lindquist TJ. The accuracy of post and core fabricated with digital technology. *J Prosthodont* 2023;32:221–226.
16. Della Bona A, Cantelli V, Britto VT, Collares KF, Stansbury JW. 3D printing restorative materials using a stereolithographic technique: A systematic review. *Dent Mater* 2021;37:336–350.
17. Tian Y, Chen C, Xu X, et al. A review of 3D printing in dentistry: Technologies, affecting factors, and applications. *Scanning* 2021;2021:9950131.
18. Chang J, Choi Y, Moon W, Chung SH. Impact of postpolymerization devices and locations on the color, translucency, and mechanical properties of 3D-printed interim resin materials [epub ahead of print 28 September 2022]. *J Prosthet Dent* doi:10.1016/j.prosdent.2022.08.018.
19. Kessler A, Hickel R, Reymus M. 3D printing in dentistry—State of the art. *Oper Dent* 2020;45:30–40.
20. Lin L, Fang Y, Liao Y, Chen G, Gao C, Zhu P. 3D printing and digital processing techniques in dentistry: A review of literature. *Adv Eng Mater* 2019;21:1801013.
21. Plotino G, Grande NM, Bedini R, Pameijer CH, Somma F. Flexural properties of endodontic posts and human root dentin. *Dent Mater* 2007;23:1129–1135.
22. Rokaya D, Srimaneepong V, Sapkota J, Qin J, Siraleartmukul K, Siriwongrungron V. Polymeric materials and films in dentistry: An overview. *J Adv Res* 2018;14:25–34.
23. Kim HS, Yang SY, Choi EH, Kim KM, Kwon JS. Adhesion between epoxy resin-based fiber post and dental core resin improved by non-thermal atmospheric pressure plasma. *Appl Sci* 2020;10:2535.
24. Daneshkazemi A, Davari A, Askari N, Kaveh M. Effect of different fiber post surface treatments on microtensile bond strength to composite resin. *J Prosthet Dent* 2016;116:896–901.
25. de Sousa Menezes M, Queiroz EC, Soares PV, Faria-e-Silva AL, Soares CJ, Martins LRM. Fiber post etching with hydrogen peroxide: Effect of concentration and application time. *J Endod* 2011;37:398–402.
26. Asmussen E, Peutzfeldt A, Sahafi A. Bonding of resin cements to post materials: Influence of surface energy characteristics. *J Adhes Dent* 2005;7:231–234.
27. Dantas MCC, do Prado M, Costa VS, Gaiotte MG, Simão RA, Bastian FL. Comparison between the effect of plasma and chemical treatments on fiber post surface. *J Endod* 2012;38:215–218.
28. Valandro LF, Yoshiga S, De Melo RM, et al. Microtensile bond strength between a quartz fiber post and a resin cement: Effect of post surface conditioning. *J Adhes Dent* 2006;8:105–111.
29. Leme AA, Pinho AL, de Gonçalves L, Correr-Sobrinho L, Sinhorette MA. Effects of silane application on luting fiber posts using self-adhesive resin cement. *J Adhes Dent* 2013;15:269–274.
30. Prado M, Marques JN, Pereira GD, da Silva EM, Simão RA. Evaluation of different surface treatments on fiber post cemented with a self-adhesive system. *Mater Sci Eng C* 2017;77:257–262.
31. Liu C, Liu H, Qian YT, Zhu S, Zhao SQ. The influence of four dual-cure resin cements and surface treatment selection to bond strength of fiber post. *Int J Oral Sci* 2014;6:56–60.
32. Balbosh A, Kern M. Effect of surface treatment on retention of glass-fiber endodontic posts. *J Prosthet Dent* 2006;95:218–223.
33. D’Arcangelo C, D’Amario M, Vadini M, De Angelis F, Caputi S. Influence of surface treatments on the flexural properties of fiber posts. *J Endod* 2007;33:864–867.
34. Choi Y, Pae A, Park EJ, Wright RF. The effect of surface treatment of fiber-reinforced posts on adhesion of a resin-based luting agent. *J Prosthet Dent* 2010;103:362–368.
35. Valdivia ADCM, Novais VR, Menezes MdS, Roscoe MG, Estrela C, Soares CJ. Effect of surface treatment of fiberglass posts on bond strength to root dentin. *Braz Dent J* 2014;25:314–320.
36. Küden C, Karakaş SN. Photodynamic therapy and gaseous ozone versus conventional post space treatment methods on the push-out bond strength of fiber posts luting with different resin cements. *Photodiagnosis Photodyn Ther* 2021;36:102586.
37. van Oss CJ, Chaudhury M, Good RJ. Monopolar surfaces. *Adv Colloid Interface Sci* 1987;28:35–64.
38. Asmussen E, Peutzfeldt A. Resin composites: strength of the bond to dentin versus surface energy parameters. *Dent Mater* 2005;21:1039–1043.
39. Yenisey M, Kulunk S. Effects of chemical surface treatments of quartz and glass fiber posts on the retention of a composite resin. *J Prosthet Dent* 2008;99:38–45.
40. Vano M, Goracci C, Monticelli F, et al. The adhesion between fibre posts and composite resin cores: the evaluation of microtensile bond strength following various surface chemical treatments to posts. *Int Endod J* 2006;39:31–39.
41. Elsaka SE. Influence of chemical surface treatments on adhesion of fiber posts to composite resin core materials. *Dent Mater* 2013;29:550–558.
42. Alshahrani A, Albaqami M, Naji Z, et al. Impact of different surface treatment methods on bond strength between fiber post and composite core material. *Saudi Dent J* 2021;33:334–341.
43. Ferrari R, Attin T, Wegehaupt FJ, Stawarczyk B, Tauböck TT. The effects of internal tooth bleaching regimens on composite-to-composite bond strength. *J Am Dent Assoc* 2012;143:1324–1331.
44. Tao L, Pashley DH. Shear bond strengths to dentin: effects of surface treatments, depth and position. *Dent Mater* 1988;4:371–378.
45. Vieira C, Bachmann L, Chaves CDAL, Silva-Sousa YTC, Da Silva SRC, Alfredo E. Light transmission and bond strength of glass fiber posts submitted to different surface treatments. *J Prosthet Dent* 2021;125:674.e1–e7.